

Chapter 1: Introduction

For centuries, scientists have been puzzled about how Antarctic species could survive temperatures below 0°C. It wasn't until the late 1960s when Dr. Devries and Dr. Wohlshag isolated the first Antifreeze Protein (AFP) in the blood of Antarctic fish, which would open a new realm of antifreeze research¹. It wasn't long after from the 1980s to the early 1990s when teams of leading biologists discovered such proteins in a plethora of other organisms, such as insects, bacteria, fungi, and plants¹. These libraries of AFPs have unique structures and sequences that enable them to absorb to the surface of ice and prevent further ice propagation, which renders them some of the world's most effective antifreeze agents. By extension, AFPs have the potential to prevent cell damage for food and a multitude of cryopreservation applications. AFPs function by absorbing onto the surface of ice². In between sites with absorbed AFPs, the ice will grow in such a way that it will develop a highly curved surface, which will result in an extremely energetically unfavorable configuration for ice growth. Consequently, this will arrest the formation of further ice nuclei². Although promising, natural AFPs are held back by their scalability issues and lack of fundamental research concerning their ice binding mechanisms and the chemical/physical features that help suppress ice growth. In this research, we aim to design several antifreeze mimetics in the form of antifreeze peptides to help us further our understanding on the physical and chemical attributes that are necessary in the suppression of ice growth and in addition, expand the usage of such mimetics by making potential anti-ice coatings.

1.1 Major Applications

AFPs have many potential and current uses in the food and cryopreservation industries.¹ Cryopreservation is the process in which biological materials (human and nonhuman related) are stored in frozen conditions to preserve their shelf life, which is extremely important for medical and biological research fields¹. Despite current innovations, there are a multitude of issues that come with cryopreservation. Most of the time, preservatives, such as DMSO (dimethylsulfoxide) and glycerol are used to inhibit ice growth. In particular, a key property of DMSO is that it makes the cell membrane much more permeable, which contributes to decreasing the rupturing of cells via ice damage. However, the main issue with DMSO and other cryopreservatives is the

development of cytotoxicity¹. The prevention of ice growth during the thawing process is key, but in order to do so, high concentrations are needed. These high concentrations can sometimes in the long run breed toxicity within a cell line, and this is where AFPs can serve as a potential alternative solution. Most AFPs used for cryopreservation studies have derived from fish AFPs. They are not only less toxic than the mentioned cryopreservatives above, but they are much more potent at lower concentrations on the microliter level¹. There have been multiple studies conducted that demonstrate the power of AFPs in this line of work. Such examples include successful, prolonged storage of sheep embryos, hearts for organ transplants, bull sperm, rice embryonic cells, and more¹.

Along with cryopreservation, AFPs have great potential to effectively store food and prevent ice damage to crops³. They have even been used in commercial ice creams to prevent ice growth during the thawing process, which is known as ice recrystallization. As frozen ice cream is left out to thaw, this can lead to the growth of larger crystals over time. For ice cream to have its desired creamy texture, the ice crystals must remain small; if they are left to grow, it can lead to an undesired gritty like texture. AFPs can prevent the development of a gritty texture by minimizing ice growth and, thus, maintain the small size of ice crystals³. Likewise, AFPs can also be used for the storage of frozen meat. Once more, we have the motif of ice damage to cells, which consequently leads to undesired textures or even cell death. Typically, sucrose and sorbitol are used to promote long term storage of frozen meats and although they perform relatively well for preservation, they can leave an undesired sweetness within the meat. Again, these proteins have been investigated to resolve such issues for meats and fish alike³. For example, AFPs have been used to successfully prevent ice damage to lamb meat, but they must be injected before slaughtering to make it highly effective³. Besides storing frozen food, AFPs can also be utilized in agriculture as well. Many biologists and geneticists have conducted studies to express AFPs in other species of animals and plants to improve their freeze tolerance. Such common examples include using fish AFPs to promote freeze tolerance in many different species of tomatoes, potatoes, tobacco, and even salmon eggs³. In particular, ice recrystallization inhibition has been successfully embedded in the leaves of tomato plants³.

Natural AFPs have been shown to be powerful in applications relating to cryopreservation, food, and agriculture. Although exciting, these highly studied, natural AFPs

pose major scalability issues. In all of these studies, only small amounts of these proteins are able to be drawn from such organisms, which is not only time consuming but also makes them unfeasible for industrial level uses. Likewise, they are also prone to degradation issues as well^{1,3}. To overcome such obstacles, researchers over the past few decades have collected libraries of AFPs to use as inspiration for the development of Antifreeze Protein Mimetics (AFPMs). Many of these AFPMs consist of synthesized peptides and synthetic polymers. Not only have these AFPMs shown promising results, but they can also be further pushed for other applications that otherwise natural AFPs would not be suitable for. For instance, there have been some studies conducted that looked into using these mimetics as potential antifreeze coatings. Studies by Koshito and Zhang et al. have anchored short peptides and polypeptides to substrates that showed anti icing capabilities. This can potentially open the window for AFPM anti-ice coatings.^{4,5} Hopefully by improving upon the robustness and scalability of their design, the potency of AFPMs akin to those of natural AFPs and be used for further applications to prevent ice damage in many different industries.

1.2 Ice Nucleation Background

To comprehend how AFPs bind to ice, ice nucleation (IN) and crystallization is essential to understand first. It is important to distinguish that crystallization is separate from nucleation. Crystallization is driven when there is a chemical potential difference between an ambient phase and a crystalline phase in which the ambient chemical potential is higher than the latter. Ice crystallization, in particular, is driven by the degree of supercooling or extent to which the solution freezes below its melting point⁷. However, crystallization cannot occur without a nucleation event. IN can only occur when it reaches or surpasses an energy barrier as shown in Figure 1. Once this energy is overcome, the ice nucleus is said to reach its critical radius, which is the size in which the nucleus is thermodynamically stable⁸. Depending on the kind of IN that occurs, this barrier can be higher or lower. For instance, homogenous IN is the freezing of water without the presence of any foreign body or particle, and this results in a higher nucleation activation barrier. In this mode of IN, there is a competition between two key factors. On one hand, there is decreasing free energy of the system by the development of a crystal but on the other, there is an energy penalty associated with the formation of a surface. Overall, we want the decreasing free energy of the crystal to override in order for nucleation to happen. Homogenous IN can be quantified via Equation 1⁹.

$$\Delta G_{Homo}^* = \frac{16\pi\gamma_{cf}^3}{3(\rho_c\Delta S_m\Delta T)^2}$$

Eq 1. This equation quantifies the homogenous ice nucleation barrier. Here, ρ_c represents particle density of the ice nucleus , γ_{cf} is the surface free energy area density of the crystal and the fluid phase, ΔS_m is the melting entropy per molecule, and ΔT the degree of supercooling⁹.

When a foreign body, such as a dust particle or a wall container is introduced, then this energy barrier can actually decrease, which leads to heterogeneous IN⁷. The extent of this decrease can be defined via the function in Equation 2, which is the ratio between the energy barrier for heterogeneous IN and homogeneous IN. An important result that can be derived from Equation 2 is the effect that a curved versus flat substrate has on IN (Figure 2). In essence, when there is a large curvature to the substrate that is greater than that of the ice nucleus, then the nucleus will become unstable. This results from an increase in the chemical potential at a curved versus flat surface since it is exposed to a higher vapor pressure. Consequently, the ice nucleus that will develop on top of this surface needs more energy to form or further supercooling to exist, which makes it more thermodynamically unstable. The need for a higher degree of driving force for an ice nucleus to develop on top of a highly curved surface is known as the Gibbs Thomson Effect⁹. This is an important phenomenon because this is how AFPs work. AFPs will bind to ice in such a way that it will force the ice to grow with a highly curved surface. Because this curvature is thermodynamically unfavorable, it will push for inhibition of further ice growth.

$$f(m, R') = \Delta G_{Heter}^* / \Delta G_{Homo}^*$$

Eq 2. This function, also known as the interfacial correlation factor, can quantify the change in the energy barrier when heterogeneous IN is induced. The m represents the contact angle between the nucleus as well as the interfacial free energy between a substrate and the fluid phase, substrate and crystalline phase, and finally the crystal phase and fluid phase. R' denotes the normalized interfacial structure size of said substrate or foreign body.

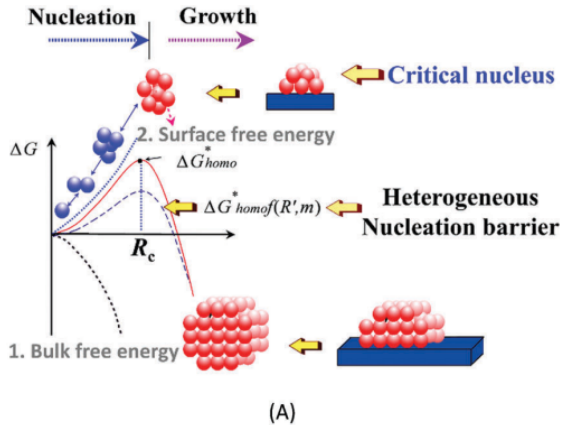


Fig 1. Above demonstrates the kinetic energy barrier that must be overcome in order for ice nucleation to take place. With the addition of a substrate, this barrier can decrease, and this is known as heterogeneous ice nucleation⁸.

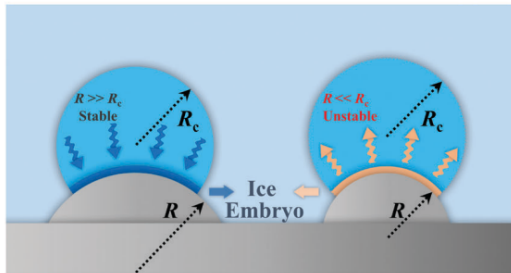


Fig 2. This schematic shows the effect of a curved substrate. If the curvature of the substrate is much greater than that of the critical ice nucleus radius, then the ice nucleus will become unstable. As a result, no further ice will grow. This is once again known as the Gibbs Thomson Effect.

1.3 Natural Antifreeze Proteins

There is a large gamut of AFPs that have been detected across many different species. Thanks to the work of several leading biologists, much of the AFP's structures and amino acid sequences have been uncovered. The main feature between all natural AFPs is their ability to bind to a particular ice plane, which most of the time consists of the basal and primary prismatic planes (Figure 3)¹¹. All AFPs bind to the surface of ice at a specific site known as the ice binding site (IBS). One common feature that strings all these types of AFPs together is the fact that IBS are generally flat/rigid and have some kind of hydrophobic character¹⁰. However, the role of this hydrophobic character was not realized until much later down the road. Originally, many researchers supported that AFPs binded to ice via hydrophilic groups, such as hydroxyl groups¹². This, in particular, was modeled by the threonine residues found in several types of AFPs

because threonine (as shown in Figure 3) contains a hydroxyl side chain. Specifically, it was suggested that binding could occur due to distance matching between the hydroxyl groups of the threonine and the oxygen atoms in the basal or prismatic plane of ice (Figure 4). This would result in hydrogen bonding between said groups, thus leading to irreversible binding¹². Although not completely wrong, this model disregards the importance of hydrophobic groups, which was realized once mutation studies on AFP Type I (AFPs that are alanine rich) emerged.¹³ Mutation studies of AFPs have been critical in helping to better understand the ice binding motifs of AFPs. These kinds of experiments alter the amino acid sequences of these proteins, which has elucidated the roles of hydrophobic and hydrophilic groups on the ice binding mechanism of these proteins. For instance, studies on AFP Type I replaced a threonine with other amino acids such as valine, alanine, and serine (more hydrophobic groups) and from there, scientists have recognized a big change in antifreeze properties, which suggested that hydrophobicity plays a crucial role¹³. There is still much work in terms of simulation and experimental studies to be done to unravel the many still unknown structures of AFPs and their specific features, such as the planes of ice to which they bind. With that being said, simulation studies have led researchers to uncover that AFPs are not only diverse in their structure and sequences but also in their ice binding mechanisms¹¹.

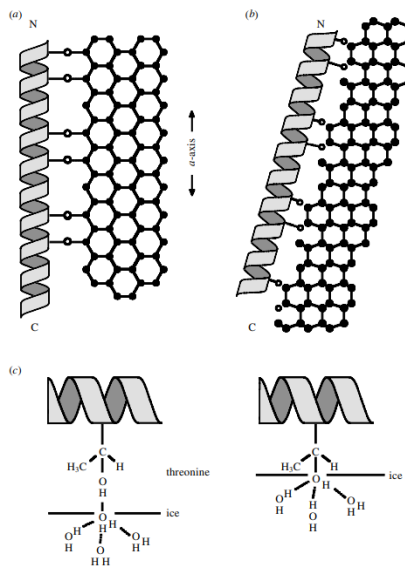


Fig 3. This schematic shows the distance matching model. In a and b, the hydrophilic groups of the peptide, represented by the coil, can hydrogen bond with the hydrogen atoms of a given ice plane (the two different orientations of the lattices represent two different planes of ice). Subfigures c and d are meant to

highlight the extent of hydrogen bonding. It was thought originally that hydrogen bonding can only occur above the surface of ice, but in more recent years, it is possible for the hydrophilic group of the peptide to go inside the ice and induce hydrogen bonding from there¹¹.

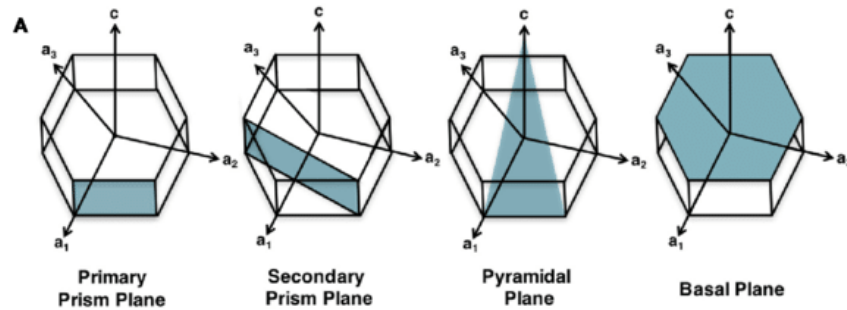


Fig 4. These are the four planes of hexagonal ice. Most AFPs according to literature attach themselves to the basal or primary prism plane although attachment to the primary prism plane is more common⁸.

1.3.1. Fish AFPs

Fish AFPs have been extensively studied in literature and can be broken down into Types I-IV and Antifreeze Glycoproteins (AFGPs) based on their sources and helical structure¹⁰. The structures of all types are highlighted in Figures 5 and 6. Type I AFPs have an α -helical structure and are classified further into three different types depending on their size and genetic makeup. They have an overall amphipathic structure with an IBS that has a certain degree of hydrophobicity¹⁰. Most of their amino acid sequence is composed of alanine and most notably has three repeats of Thr-Ala-Ala-X-Ala-X-X-Ala-Ala-X-X where Ala is alanine, Thr is Threonine, and X is an arbitrary amino acid³. Type II AFPs are cysteine rich globular (circular-like) proteins that contain five disulfide bonds¹². Like Type II, Type III proteins are also globular but on a larger scale (around 6kDa). Type IV AFPs are rich in glutamate and glutamine and have alpha helices that are unrelated to the other types of AFPs¹³. Finally, AFGPs provide a more interesting case: They are much more flexible compared to Types I-IV AFPs and contain a tripeptide repeat of Ala-Ala-Thr with disaccharide side chains. When binding to water, studies have shown that it adopts a type II polyproline helix¹³.

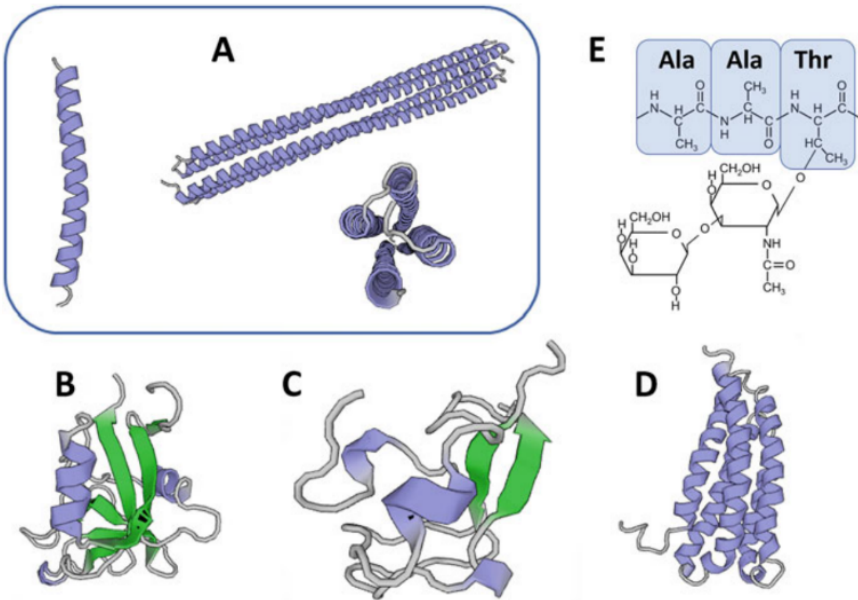


Figure 5. A-D represent common structures found in AFP Types I-IV in this order respectively. The gray represents the peptide backbone, the green represents a β -helix, and the blue is an α -helix. Structure E represents the AFGP.¹⁰

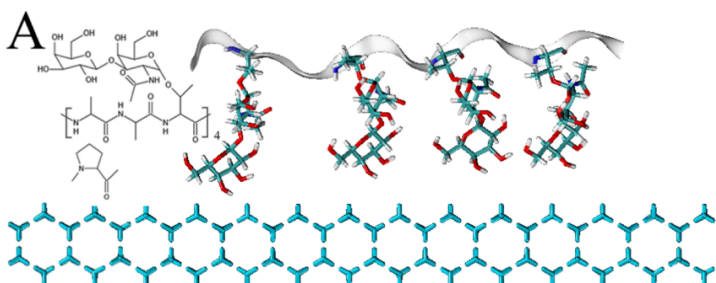


Figure 6. Above is a close up of the structure of AFGP, which adopts a type II polyproline helix. It contains a peptide backbone with disaccharide side chains and methyl residues from its amino acids¹³.

1.3.2. Insect AFPs

In contrast to fish AFPs, many insects, winter plants, and bacteria are rich in having a beta helical structure as shown in Figure 7². In particular, AFPs from insects will be highlighted in great detail as they will serve as our primary source of inspiration for making our very own AFPM. Insect AFPs are of interest because they are much more potent than fish derived AFPs¹⁴. In fact, studies have shown that they can be four times more active than fish AFPs¹⁴. Most notably, Dr. Peter L. Davis is a leading figure in the uncovering of many AFP structures and is credited along with his team members to discover and present the structures of many key insect

AFPs- most notably from the spruce budworm (*Choristoneura fumiferana*)¹⁴ and beetle *Tebebrio molitor*¹⁵. The spruce budworm's structure consists of a left handed β -helix (similar to Figure 7a)¹⁴. Its IBS consists of a residue motif of four Thr-X-Thr sequences where Thr once again is threonine and X is any inward pointing amino acid¹⁴. The beetle AFP is shown in Figure 7a and its architecture consists of a parallel β -helix structure with 12 amino acid loops¹⁵. It is rich in threonine and cysteine, and in a similar fashion to the spruce budworm, the beetle TmAFP has a Thr-X-Thr motif where in this case the X represents cysteine¹⁵. Compared to the structure of previous fish AFPs, the architecture of insect AFPs is much simpler and contains more repetitive patterns in their amino acid sequences. This makes them an ideal model for designing AFPMs along with their immense anti-freezing potency. Lastly, it is important to highlight that insect AFPs as well as some fish AFPs contain threonine at their IBS. This is suggested by numerous studies that the threonine amino acid plays a large role in the ice binding motif, which will be and further elaborated on in the next section.⁹⁻¹²

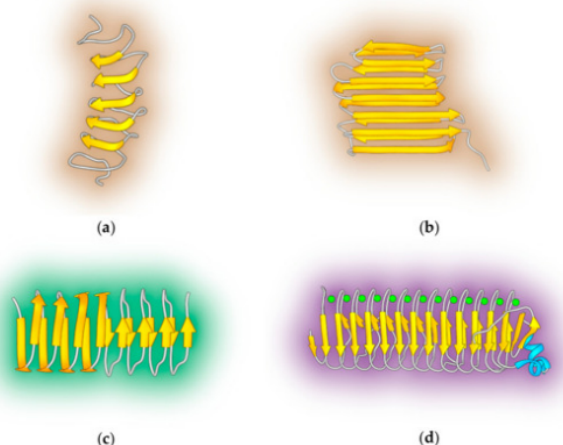


Fig 7. β -helical AFPs deriving where a-b are from insects, c from ryegrass, and d from bacteria²

1.3.3. Ice Binding Motifs

As discussed in the previous sections, AFPs and AFGPs are rich in diversity when it comes to architecture and sequence patterns. This wonderful variety is also shown in their ice binding motifs. To reiterate, the original model for ice binding motifs of AFPs consisted of an exclusive hydrogen bonding theme between the hydrophilic groups of the AFPs and that of the oxygen atoms in a particular plane of ice. With emerging simulation and mutation studies, we

have expanded our understanding on how AFPs bind to ice and have come to recognize that the nature of such absorption is much more intricate than ever anticipated. More importantly, we have learned that hydrophobicity plays a key role in the story. This is still a newly birthed emerging field that is only a few decades old, and so there is still much more work to be done. The binding motifs of AFP Types II and IV are extremely complex and more simulation studies are needed. For the sake of clarity and relevance, the ice binding motifs for AFGPs, AFP Type and III, and insect AFPs will be highlighted in this section.

As mentioned previously, hydrophobicity plays a key role, but there are, in fact, AFPs that bind exclusively via hydrophobic groups (typically methyl groups). These groups consist of AFGPs, AFP Type I, and AFP Type III.^{16,17} For Type I AFP, which typically derives from winter flounder, its IBS contains Ala-Ala-Thr repeats. The methyl groups pointing out from alanine and threonine have been proposed to match distances to those of ice grooves, which results in absorption¹⁴. Contrary to Type I, Type III has no threonine repeats, but has a similar ice binding motif. In one simulation study conducted by Chakraborty et al., Type III AFP was studied and some noteworthy findings were observed¹⁷: First, it was confirmed that hydrogen bonding to ice is not a factor in its ice binding motif. This was supported with observations from the simulation that paralleled experimental evidence in which the AFP has a preference for pyramidal and prism planes and not the basal plane at all. This is significant because the basal plane has the potential to form the most hydrogen bonds whereas the pyramidal plane has the least¹⁷. Likewise, this was further corroborated in simulations that showed the methyl groups facing the ice surface and polar groups away. What these hydrophobic groups do is actually initiate the ordering of water molecules via hydrophobic interactions. This then results in the formation of water cages around the IBS, which is mainly hydrophobic (See Figure 8). These water cages are then able to anchor the IBS to the pyramidal plane¹⁷. In fact, the ordering of the water molecules to this plane matches quite well.

Although binding via only hydrophobic groups, AFGPs operate in a slightly different mechanism from Type I and Type III AFPs. In comparison to these two groups, AFGPs are actually much more flexible, which left many scientists originally puzzled, but simulation studies conducted by Molinero et al. have shed light to the matter on AFGP8¹³. As previously mentioned, the AFGP has a type II polyproline helix, and this particular conformation plays an important role in its ice binding motif. This configuration allows for the right separation of

methyl groups between its disaccharide and amino acid hydrophobic residues to allow for distance matching of these hydrophobic groups to the cavities of the primary prismatic plane (Figure 9). This once again mirrors the motif in Type III AFPs, but in this case, there is added flexibility that comes into play.¹³ Due to this decrease in rigidity, the AFGP is able to walk (in a similar fashion to an inchworm) until it bumps into a cavity where its hydrophobic groups can then absorb into the ice¹³.

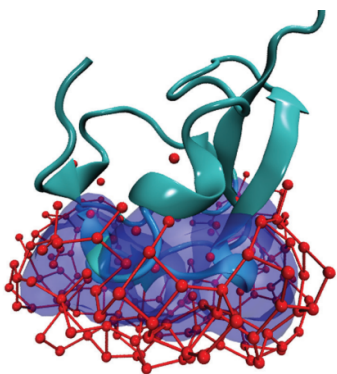


Fig 8. Here shows the binding motif of AFP Type III. The turquoise is the non IBS of the protein and the blue represents the IBS. The red balls represent the water molecules and the red sticks are the hydrogen bonding network. We see that the hydrophobic IBS is completely encapsulated by the water molecules¹⁷.

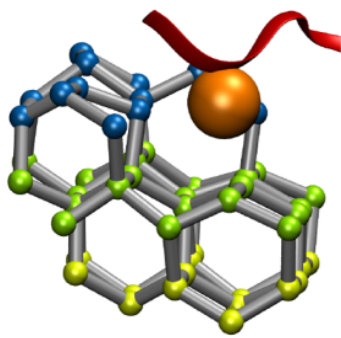


Fig 9. The peptide backbone is represented in red and the orange ball correlates to a methyl group being absorbed into a kink or cavity of the ice lattice, which is hexagonally shaped¹³.

When it comes to the insect AFPs as mentioned before, both hydrophilic and hydrophobicity play a key role in its ice binding mechanism. As mentioned before, these AFPs have a β -helix architecture that allows for the Thr-X-Thr to align itself as a flat array. What this results in is the distance matching between the hydroxyl groups of the threonine to the oxygen atoms of the basal and primary prismatic planes¹⁴⁻¹⁷. When it comes to the hydrophobic groups

or methyl groups of the threonine, their role has become much clearer thanks to simulation experiments. To untangle such roles, simulation studies by Molinero et al. on TmAFP were conducted in which certain amino acids were exchanged with threonine that contained either more hydrophobic or hydrophilic side chains. This is done in a similar manner to mutation studies only in simulation form.¹⁸ One major role that resulted from such study is that the methyls are key to increasing rigidity at the IBS¹⁸. Again, we see that flatness of the IBS is key for the AFP to successfully bind to ice. This was observed when certain threonines were replaced with serine, which has no methyl groups in its structure. Upon such mutation, this added a degree of flexibility that weakened binding to ice¹⁸. Next, the methyls are needed to stabilize the ice binding motif known as anchored clathrate (AC) ice binding.^{16,18} In this part of the study, methyl groups were deleted on the long and short side of the IBS by again mutating a threonine to serine. Deletion on the short side resulted in the formation of empty clathrate cages, which are thermodynamically unstable while deletion on the long side resulted in the degradation of such cages. Consequently, methyl groups are needed to stabilize such water cages and in tangent, these cages are actually anchored via the hydroxyl groups of the threonine residues.^{16,18} The special thing about this AC motif is that it allows for the absorption to multiple ice planes as shown in Figure 8 as well. Moreover for AFGPs and Type I AFPs, hydrophobic dehydration acts as a major driving force for binding, but for insect AFPs, it does not. As discussed previously, methyl groups are able to be absorbed into the cavities of ice (Figure 10). This leads to the loss of water molecules at the ice surface, which naturally increases entropy, but this is not the case for insect AFPs: For these proteins, the methyl groups do not exactly go into the holes or grooves of ice directly. Instead, they organize the water at the ice-water interface into these cages that then allows for binding to facilitate.¹⁸. Alongside methyl groups, the hydroxyl groups of the threonine play one more important role to this ice binding mechanism. In the structure of such insect AFPs, there is the presence of a trough between two rows of threonines where water molecules are stuck in between. This results in the formation of a water channel. The immobilization and ordering of this water has been found to be key in helping to order the remaining water for the formation of the AC motif¹⁸. However, more recent studies have challenged this prerequisite and so further study is needed in this area¹⁹.

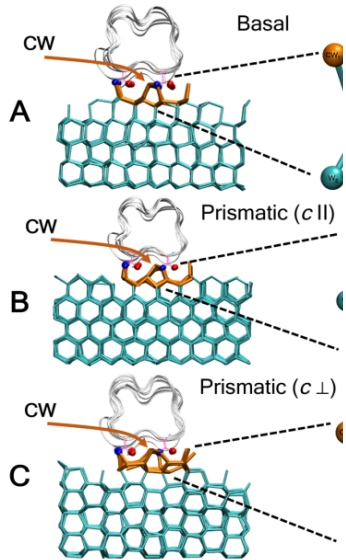


Fig 10. Above highlights the anchored clathrate (AC) motif of insect AFPs. This can occur for different planes of ice. In these images, the turquoise sticks and balls represent the ice lattice, the orange sticks represent the AC motif, and the red and blue balls are the hydroxyl and methyl groups of the IBS¹⁸.

Despite differences in structure, amino acid repeats, and ice binding mechanisms, there are some key insights that are shared amongst the majority of these AFPs. Distance matching between residues of the IBS and ice lattice are a must but this goes hand in hand with the structure of the IBS itself. All IBS have a hydrophobic component, which is important not only for structural rigidness, but also for facilitating ice binding. Methyls have been shown to orient the AFPs in the correct manner to bind and provide a more stiffer binding site. Furthermore, there is no doubt that threonine plays a key role in the AFP sequence, and it has been shown with many of these AFPs that its methyl and hydroxyl groups are important to effective ice binding. The important synergistic effect between hydrophobicity and hydrophilicity is one that will be extensively studied for the design of AFPMs because as shown above, both can play a major role in allowing the AFP to bind to the ice surface.

1.3 AFP Effects

Upon binding, AFPs can have two main effects: thermal hysteresis (TH) and ice recrystallization inhibition (IRI)²⁰⁻²². Similar to the Gibbs Thompson effect, the absorption of the AFP will force ice nuclei to grow in between AFP binded sites, which results in highly curved ice nuclei (Figure 11). Once again, this high curvature is not thermodynamically stable and as a result, this will

inhibit further ice formation. This is known as the Kelvin Effect²⁰. An important consequence of this effect is the depression of the freezing point without having an effect on the melting point. The reason why the freezing point decreases is because in order to stabilize such an ice nucleus, further supercooling is mandated. In other words, for ice nucleation to occur, the system needs to be cooled to lower temperatures. This gap between the melting and freezing point is known as thermal hysteresis (TH) and the more potent the AFP, the larger the gap.²⁰

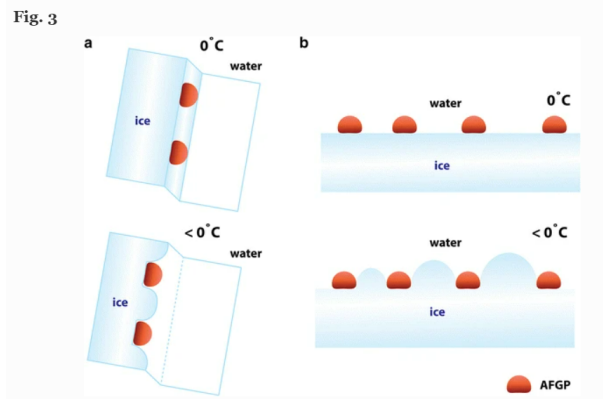


Fig 11. Upon absorption, the AFP will bind to ice and drive ice to grow in an unstable, high curvature configuration that then induces a freezing point depression phenomena known as thermal hysteresis.

In addition to TH, AFPs are known to also induce ice recrystallization inhibition (IRI). Ostwald's Ripening is a common event that is driven by an inhomogeneous solution. Essentially, smaller particles tend to have a higher surface energy than larger particles in this solid-liquid system, and so in order to decrease the energy of the entire system, the particles begin to grow over time to diminish its surface energy. In the context of this application, Ostwald's Ripening occurs when ice in an already polycrystalline sample begins to thaw. AFPs have the ability to slow this growth as shown in Figure 12, which results in smaller crystals over time. One important nuance to note is that Ostwald's Ripening on a microscopic scale represents the diffusion of water molecules that travel from an ice crystal with a higher curvature to one of lower curvature (smaller to larger ice crystal). It does not take into account the growth of ice crystals due to accretion or the process in which two ice crystals make contact with one another, which results in a larger crystal (Figure 12).²¹⁻²² In addition, AFPs and AFPMs have also shown to change the spherical shape of an ideal ice crystal to that of a fractal like pattern, which visually shows ice binding inhibition (Figure 13)²².

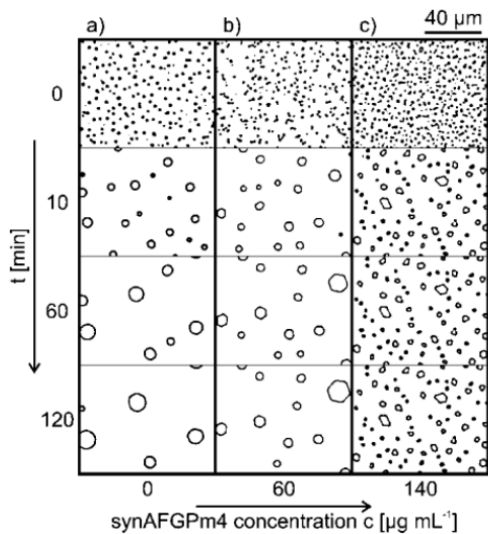


Fig 12. These images demonstrate the phenomenon of Ostwald’s Ripening and its inhibition. A 45 wt% sucrose solution was used as the control (left most column) and AFPs were added at various concentrations to observe any IRI effects (middle and right most columns). The leftmost column represents Ostwald’s Ripening where larger crystals are grown over the expense of smaller ones and as we increase concentration of the AFP, the crystals over time grow at a slower rate²¹.

AFP effectiveness is tested based on its ability to produce a TH gap, change the morphology of ice crystals, and or prevent ice recrystallization from occurring. Therefore, these parameters will be analyzed to test the effectiveness of our proposed AFPM that will be inspired by insect AFPs. More detail regarding how to quantify and analyze such events will be explained in greater detail in the methods section of this thesis.

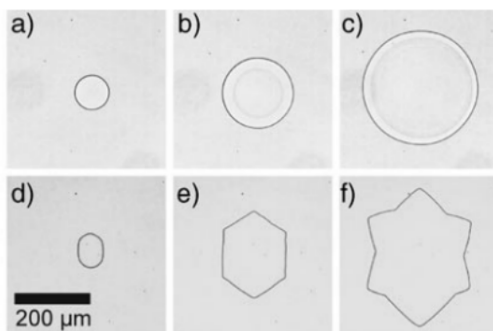


Fig 13. Typical ice crystals are spherical but once an AFPM was added, the ice crystal’s morphology completely alters. Panels a, b, and c show Ostwald’s ripening without AFP. Notice here the shape of the crystals are spherical. Panel d, e, and f shows Ostwald’s ripening in the presence of an AFP. Areas of indentation indicate sites where the AFPM has binded to ice, and thus, inhibited ice growth²².

1.4 Current AFP Mimetic Research

Thus far, we have discussed the effectiveness, structures, and ice binding motifs of many natural AFPs. However, as mentioned above, the applications of AFPs are limited by scalability issues. To mimic the very function and effectiveness of these AFPs is key here and although such inspired designs are currently limited in literature, there is much potential to access in this endeavor. The booming of AFPM research can be attributed to a famous study done by Knight et al. who discovered that many synthetic polymers, most notably PVA (polyvinyl alcohol), has anti freezing properties.²³ PVA is especially efficient in IRI and has been considered the most potent synthetic IRI agent in the world.²⁴ PVA is an attractive candidate for the design of AFPMs because of its widespread availability, low cost, and low toxicity²⁴. The exact ice binding mechanism of PVA was originally a bit of an anomaly because it broke a key pattern that many natural AFPs have in order to facilitate ice binding: PVA is completely flexible. In other words, it does not have a rigid ice binding site. To add even more confusion, it was found in one study that the random addition of hydrophilic and hydrophobic groups did not improve the IRI of PVA unlike how it would with mutation studies of natural AFPs²⁵. Some studies have currently conflicted opinions on whether PVA actually binds to ice or affects the structure of the water close to the surface of ice.²⁶ The most popular PVA ice binding motif is one developed by Budke et al. where he was the first to propose that the hydroxyls in this polymer are at the right distances to match that of the ice crystal lattice in a linear fashion.^{22,24} Although some studies still stand by Budke's model, others suggest that lattice matching is not a requirement.²⁷ Regardless, what has been experimentally observed is the IRI effectiveness of PVA is impacted by the degree of polymerization and functionalization of side chains²⁶. Overall, longer chains (degrees of polymerization up to 20) yield greater IRI activity and random acetylation does not improve upon IRI properties.²⁶ Last but not least, the anchoring of PVA onto a spherical substrate was investigated to see if it could retain IRI activity²⁸. Tuning the potential architecture of AFPMs will be useful for future industrial applications and so far in literature, many architectures such as star branched and bottle brushed PVA show no sign of IRI. In this study, PVA was synthesized via RAFT polymerization and was anchored to gold nanoparticles. To much excitement, the PVA was able to retain its IRI but under certain conditions. To stabilize the nanoparticle, the PVA chains must be long and to promote anti-freezing abilities, the density of

those PVA chains must be small on the surface of the gold nanoparticles. The low grafting density is key as the PVA molecules can move around to engage with the ice lattice versus for more constrained conformations, such star branched PVA, it is not able to find these binding sites as easily.²⁸ Overall, the discovery of PVA has proven to be a critical milestone in the design of AFPMs and will remain an important model as more simulations unravel the complex ice binding mechanism of PVA. However, PVA does have some drawbacks. One major disadvantage is that PVA can actually form a gel under freezing temperatures, which puts strain on its applicability as an IRI agent². And although it is one of the most effective antifreeze agents, it is nowhere as powerful in magnitude as AFPs or AFGPs². Moreover, PVA is not as comptable of a model to further our understanding of natural AFPs because unlike AFPs and AFGPs, PVA does not have a rigid ice binding site and is more flexible than the latter.²²⁻²⁷ Nevertheless, PVA studies do provide inspiration for developing potential peptide polymer mimetics that will also be addressed in this research as well.

The opportunity to not only further our understanding of natural AFPs but also in designing mimetics would be ideal, and this is what synthesizing antifreeze peptide mimetics can do. Designing peptide mimetics is not as well researched as PVA/synthetic polymer antifreeze agents and in addition, it offers the opportunity to play around with the amino acid sequences and side chains to see any potential effects relating to hydrophobicity, hydrophilicity, peptide length, charge, etc... A few major studies will be highlighted here regarding peptide mimetics. One major study investigated by Zhang et al. looked into making alpha helical peptides that could be made into an anti-ice surface. Here, three different alpha helix peptides with a 12 amino acid sequence were made and inspired by AFP Type 1⁵. The typical Ala-Thr-Ala scheme was maintained with some substitutions made by replacing an alanine with lysine (K), glutamic acid (E), or phenylalanine (F) as shown in Figure 14. According to an ice shaping assay, peptides 1-1 and 1-2 were able to change the spherical shape of the ice nucleus, which indicated ice binding. This was not observed for peptide 1-3 and could be due to a decrease in helicity that could affect the spacing of the threonine and alanine positions that allow for ice binding. In terms of IRI activity, only peptide 1-2 showed any signs. After preliminary tests, these peptides were attached to a substrate (polydopamine-coated surface) and anti icing tests were performed where peptides 1-1 and 1-2 showed signs of freezing point depression. Hence, only by changing the amino acid

sequences within alpha helical peptide mimetics showed promise for developing antifreeze coatings.⁵

name	amino acid sequence	molecular weight
peptide 1-1	DTASDAAAAAAL	1047
peptide 1-2	DTASDAKAAAEL	1162
peptide 1-3	DTASDAFAAAAL	1123

Fig 14. Sequences from Zhang et al. study inspired by Type I AFP.⁵

In more current studies, the design of peptoid oligomers has been investigated. Peptoids are similar to peptides except that at the alpha carbon, the side chain is transformed into nitrogen chains. An added bonus is that they are also less toxic than DMSO for cryopreservation. Inspired by the roles of hydrophobic and hydrophilic groups in natural AFPs, this research aimed to study the effects of such groups²⁹. All peptoids produced no TH gap, but did show IRI activity. In particular, those with long alkyl side chains (hence more hydrophobic groups) induced better binding and thus more IRI. This activity was also enhanced when using block components that contain both hydrophobic and hydrophilic groups, which again solidifies the importance of both components on ice binding affinity²⁹.

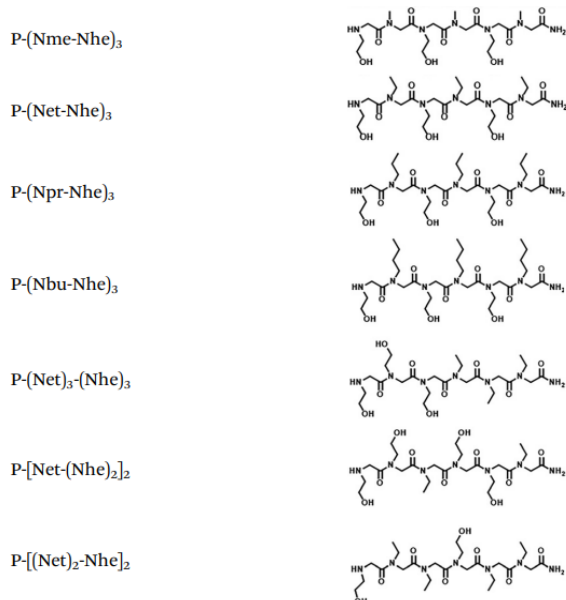


Fig 15. Different peptoid oligomers with different hydrophilic and hydrophobic side chains²⁹.

Lastly, a recent study was inspired by the threonine residues of many AFPs. Based on the methyl and hydroxyl groups of the threonine, a mimetic was designed called pHMPA with similar side chains (Figure 16)³⁰. Initial studies pointed that pThr was not enough to induce IRI until it was polymerized. Following these results, a pHMPA polymer was made and it was observed that as its molecular weight increased so did IRI activity. More notably, pHMPA with molecular weight of 45kDa induced IR acidity at concentrations less than 0.01 mg/mL, which is on the level of natural AFPs³⁰. This current study along with others supports the notion that threonine residues are important to ice binding and can serve as potential models for peptide mimetics, which will be further investigated in this proposed research.

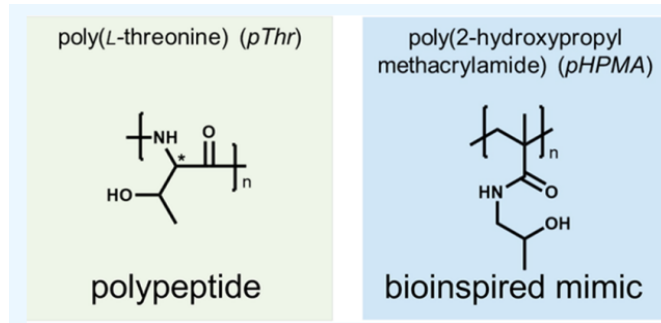


Fig 16. AFP mimetic based on threonine residues³⁰

1.5 Proposed Research

In this project, we plan to take inspiration from the IBS of insect AFPs such as TmAFP or the spruce budworm. Both of these are β -helical and the IBS is located on the β -strands in which threonine residues are exposed to the inference of water and ice. To simplify the helix, we will focus more on mimicking these β strands (Figure 17) and investigate the impact that different amino acid sequencing has on IRI and TH. Only amino acids found in natural AFPs will be investigated using a Thr-X-Thr scheme. These threonines will be spaced out in such a way that they can induce hydrogen bonding via its hydroxyls with the oxygen atoms of the ice lattice. In addition to hydroxyl groups, we are curious to see the effects that addition of hydrophobicity will have on our intended peptide and plan to increase or decrease the degree of certain hydrophobic substitutions. Overall, these libraries of peptides will be synthesized using solid state peptide synthesis. In tandem, a constrained peptide alongside a peptide-polymer conjugate will be made to investigate the role of flexibility and to what extent the IBS must be rigid (Figure 17). It is

hypothesized that this cyclization will further constrict the location of the hydroxyls on the threonine to allow better match between these hydrophilic groups to the ice plane. This more rigid peptide (cyclized) has to the best of our knowledge not been synthesized for this specific application. The synthesis pathway is similar to that shown in Figure 18. Taking inspiration from PVA polymer studies, our intended peptide-polymer conjugate will aim to see how certain properties such as peptide density and the molecular weight of the polymer play into enhancing or reducing anti icing activity. Similar to that of the Wang et al. and Stubbs et al. studies, we were inspired to anchor our peptides to both flat and spherical substrates to explore the potential of creating anti ice peptide coatings. To test the effectiveness of such peptides, peptide polymers, and anchored peptides, immersion freezing, ice recrystallization inhibition, and ice shaping assays will be utilized.

Finally, going hand in hand with these AFP ice experiments, simulation studies will be done by some of our collaborators to investigate the ice binding motif of our mimetics as well as how certain features such as peptide length, sequencing, hydrophobicity , hydrophilicity, and charge play a role in inhibiting the growth of ice. These simulations will be modeled after big leaders of the field, such as Dr. Valeria Molinero, who has conducted simulations on AFPs and PVA ice binding mechanisms, kinetics, and thermodynamics. Not much attention has been garnered towards the design of antifreeze protein mimetics, and it is an exciting endeavor that can not only serve as a simple model for AFPs but also allow for a wide range of creativity when it comes to creating potential anti-icing peptide polymers and coatings.

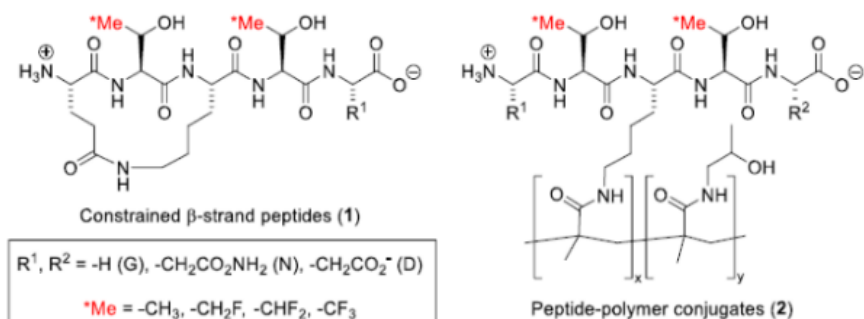


Fig 17. Proposed β strands antifreeze peptide mimetics

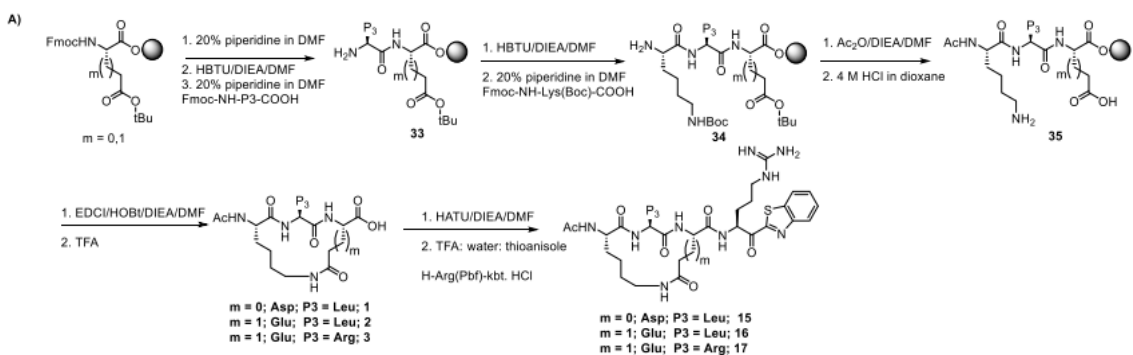


Fig 18. Similar synthesis pathway for creating cyclized peptide³¹

Chapter 2: Experimental

1. Ice Nucleation Experiments

Materials Summary

Fisherbrand Microscope Cover Slides (25 mm), Halocarbon 25-5S grease, Dow Corning high vacuum grease, vacuum O-ring, 99% purity sucrose, Ultra Pure Millipore water, Thermo Scientific D(+)-Sucrose 99+%, Sigma Alrich >99.5% glycerol, Olympus BX51 microscope, BCS 196 linkam stage, Linkam TMS 94 Stage Temperature Controller with VC 94 Vacuum Controller, Liquid Nitrogen Benchtop container, Fiber-Lite MI-LED, Cyrocon 32 temperature controller, Hitchai camera, Q imaging QiCam, Fisherbrand 1mm thick microscope slide, Northern Eclipse Software

1.1. Ice Recrystallization Inhibition (IRI)

The rate at which IRI occurs in the presence of an antifreeze protein mimetic was measured in a 17 wt% glycerol solution as well as a 45 wt% sucrose solution. A sucrose or glycerol solution must be used in order to image circular, individual ice crystals. If water was used, then there would be a flat sheet of ice versus individual ice crystals. IRI was measured using the setup shown in Figure 19. The first panel, (a), shows an entire view of the apparatus. The sample will be placed on a cooling stage, or Linkam stage. This is located on the Olympus BX51 microscope stage (white arrow). A Q imaging camera is located right above the microscope lenses in order to take images of the ice crystals. The blue arrow points to the liquid nitrogen container, which has a white tube that allows the liquid nitrogen to travel to the linkam stage, which will then cool the sample. The red arrow is pointing at two important white boxes. On the top is the stage temperature controller, which controls and sets the temperature of our cooling stage when we freeze and anneal the sample. On the bottom is the vacuum controller. A small tube connecting from the vacuum controller to the linkam stage shoots out air to prevent condensation from occurring as the sample freezes and is annealed. The image in Figure 19 panel b shows a closer view of a sample on the linkam or cooling stage that is opened. When freezing or annealing happens, the stage is typically closed with a cover to prevent any water vapor from entering the apparatus.

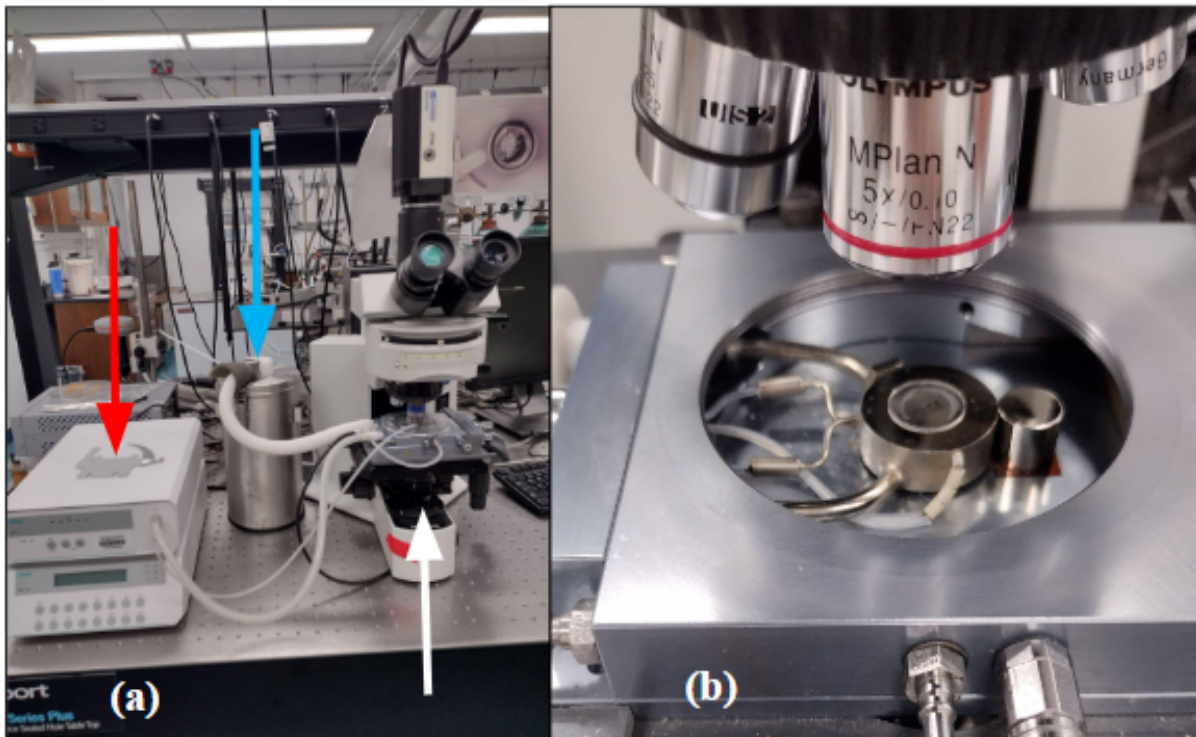


Fig 19. Panel (a) shows the entire IRI apparatus setup. Panel (b) is a close up of an example sample on the linkam stage (opened).

To calibrate the instrument, the melting temperatures of water (ultra pure Millipore water), decane, and dodecane were measured and were found to be all within 0.1K of error. The sucrose IRI experiments follow that of Budke et al. (2010)²¹ whereas the glycerol IRI experiments derived from Burkey et al. (2018)³². Sample preparation is highlighted in Figure 20. To make a sample, halocarbon grease was lined on the edges of a clean 25 mm glass cover slide. The grease is used in order to ensure that no water enters or escapes from the sample. Next, a 1.5 μL droplet of 45 wt% sucrose was dropped onto the greased cover slide. Using forceps, another 25 mm slide was placed on top of the greased slide with the sample and then pressed to create a thin sucrose film. The sucrose film was made in a way to prevent contact with the greased perimeter. A similar approach was taken with the 17 wt% glycerol sample except a 1mm microscope slide was used to replace one of the cover slides. A slide was used instead as it promoted more even heating of the glycerol sample and allowed clearer separation between the ice crystals in the glycerol solution (this was not needed for sucrose). Once samples were made, they were cooled and heated to an annealing temperature according to Tables 1 and 2. Occasionally, the melting points of the samples were measured to ensure that no water loss was observed.

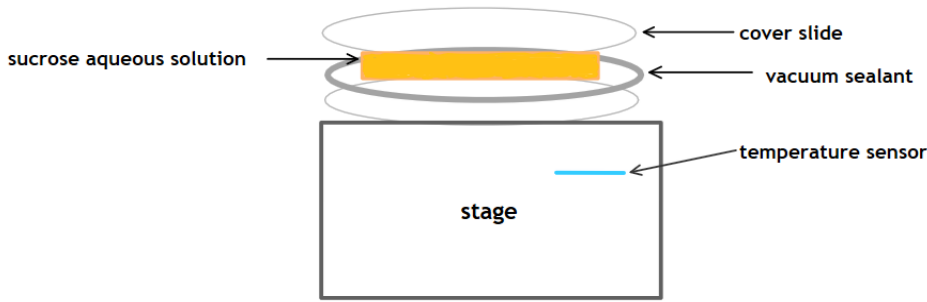


Fig 20. Schematic of sample preparation for sucrose/glycerol solution on the Linkam stage.

Table 1. 17 wt% Glycerol Cooling/Heating Rate and annealing temperature

T_0 (°C)	R_0 (°C/min)
20	30
-50	20
-6	annealing temperature

Table 2. 45 wt% Sucrose Cooling/Heating Rate and annealing temperature

T_0 (°C)	R_0 (°C/min)
20	20
-50	10
-8	annealing temperature

The above tables organize the heating and cooling rates of 17 wt% glycerol and 45 wt% sucrose systems. T_0 represents desired starting, cooling, and annealing temperatures whereas R_0 is the rate at which the sample is cooled and then heated. These temperatures and rates are based on the Budke et al. (2009)²¹ and Burkey et al. (2018)³² studies.

For image analysis, Northern Eclipse software and homemade program on Matlab was used to measure the radii of the ice crystals over time as shown in Figure 21. This was done by first taking the original image (a) and then thresholding the individual ice crystals with a red lining (b). The key in this process is to measure diffusional growth (tracking the movement of water from smaller to larger ice crystals) of the ice crystals and not accretion. Accretion is shown in the rightmost image of Figure 21 where two ice crystals grow due to touching one another. To avoid inclusion of accretional ice crystals as much as possible, the roundness, R, was used as a parameter. Roundness is defined by $R = 4\pi AP^2$ where A is the area of the crystals and P is the perimeter, and it varies from 0 to 1 (perfectly circular). To determine this criteria, we studied hundreds of ice crystals and found that crystals that grow via accretion typically have a roundness below that of 0.6, which agrees with the Budke et al. (2010)²¹ study. Northern Eclipse was used

to threshold and obtain key properties of the ice crystals, such as radius, diameter, (x,y) coordinate, area, perimeter, and roundness. A homemade program in MATLAB was developed to sort out the diffusion vs accretion growth based crystals (found at the end of the experimental section) with a more in depth description.

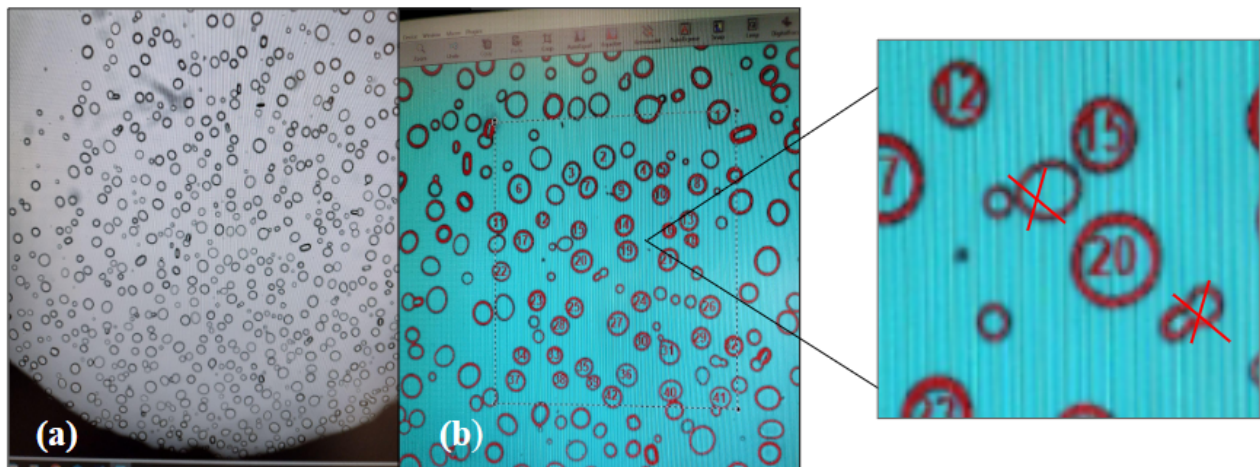


Fig 21. Using Northern Eclipse to threshold ice crystals for radius and most importantly, roundness.

1.2. Immersion Freezing

Immersion Freezing was conducted using the homemade apparatus found below in Figure 22. It has similar components to that of the ice recrystallization instrument with some modifications as shown in Figure 22. In the left image, the white arrow points to a liquid nitrogen container that has a tube coming out of it to allow flow of liquid nitrogen. The blue arrow points to a Fiber-Lite MI-LED light source used for imaging while the neon blue arrow points to the stage that contains the sample, an enclosed chamber, and Hitachi camera. Finally, the red arrow shows the Cryocon temperature controller, which is more sensitive than the one described in the ice recrystallization section. Finally, panel b shows the gaseous nitrogen trap. As mentioned previously in the IRI section, since we are cooling and heating a sample, condensation may occur and to prevent such a process from occurring we need gaseous nitrogen to combat it. This light blue bucket is connected to a gaseous nitrogen tank and to a special glassware that is being submerged in a few inches of liquid nitrogen. What this section does is ensure that no water enters this flow pathway. By cooling such glassware, water vapor is able to be trapped and, thus, prevent any possibility of

it entering in the immersion freezing apparatus. Figure 23 shows a close up of the stage while the right diagram shows a more simplified view of the stage and important functions of the apparatus.

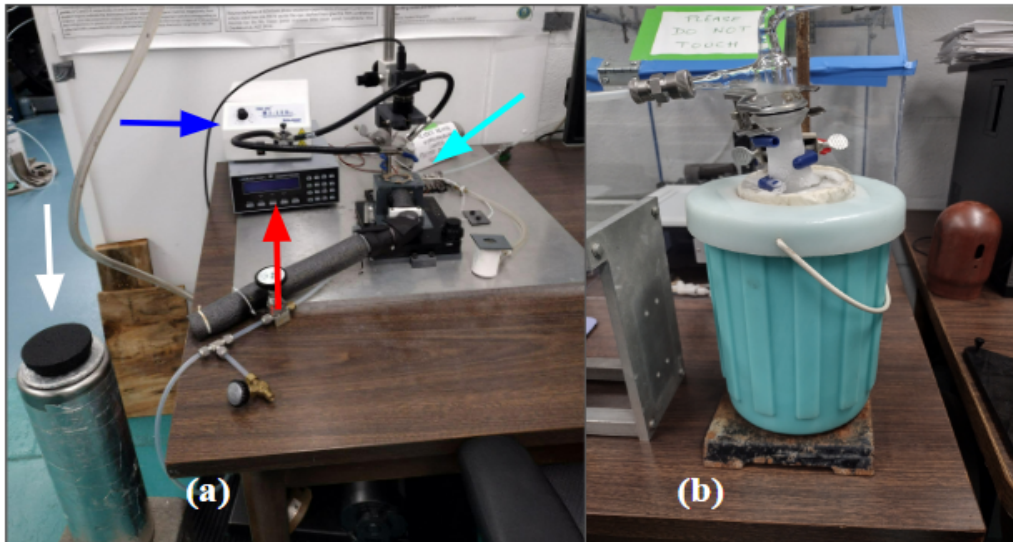


Fig 22. Panel a shows a wide view of the immersion freezing instrument. Panel b shows another component of the apparatus, which aims to allow the flow of gaseous nitrogen to prevent formation of condensation.

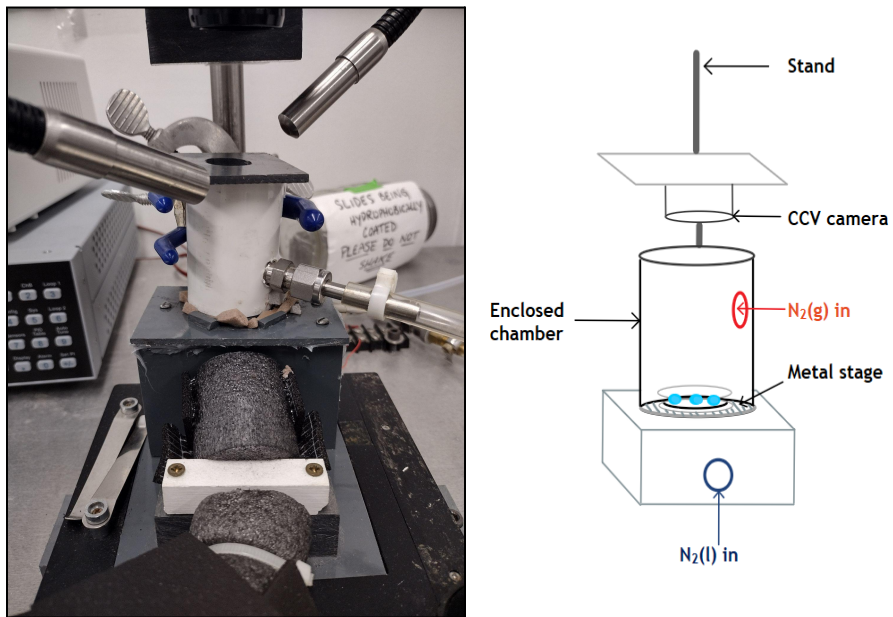


Fig 23. To the left is a close up of the homemade immersion freezing stage and on its right is a schematic showing the key components of the stage. The sample is set on a metal stage and is enclosed in a

chamber. There are ports to allow for the flow of liquid and gaseous nitrogen. Finally, a Hitchai camera is placed above to take images.

Samples were prepared in the following manner visualized in Figure 24. A clean O-ring was covered with a thin layer of high vacuum grease and then placed on the perimeter of a 25 mm glass slide. Next, 0.3 μ L droplets were placed within the O-ring making sure to not touch any grease that could tamper with freezing results. Next, another cover glass slide was placed on top and sandwiched to create the desired sample. In this case, an O-ring is used to ensure that no gas enters or escapes from or into the droplets. A real life image of the droplets is shown in Figure 25.

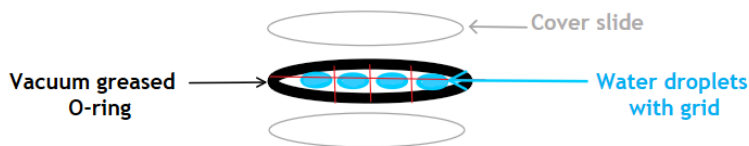


Fig 24. Above shows how a sample is prepared using a greased O-ring technique.

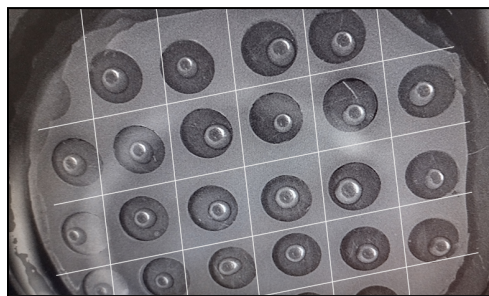


Fig 25. This is an example of an immersion freezing droplet sample.

To calibrate the apparatus, a calibration curve of the melting points of water and organics was made similar to that described in Knopf et al. (2011)³³. The melting points of water, decane, dodecane, and octane were measured and the measured vs literature melting points are illustrated in Table 3. Octane had its melting point the farthest from literature. In the set up, there is some distance between the temperature controller and the actual stage. If the stage is extremely cold, there will be a greater difference in temperature between the stage and the controller, which is at

room temperature. As a result, this change in temperature will be more sensitive for samples at lower temperatures than at higher temperatures, which is what is seen with octane.

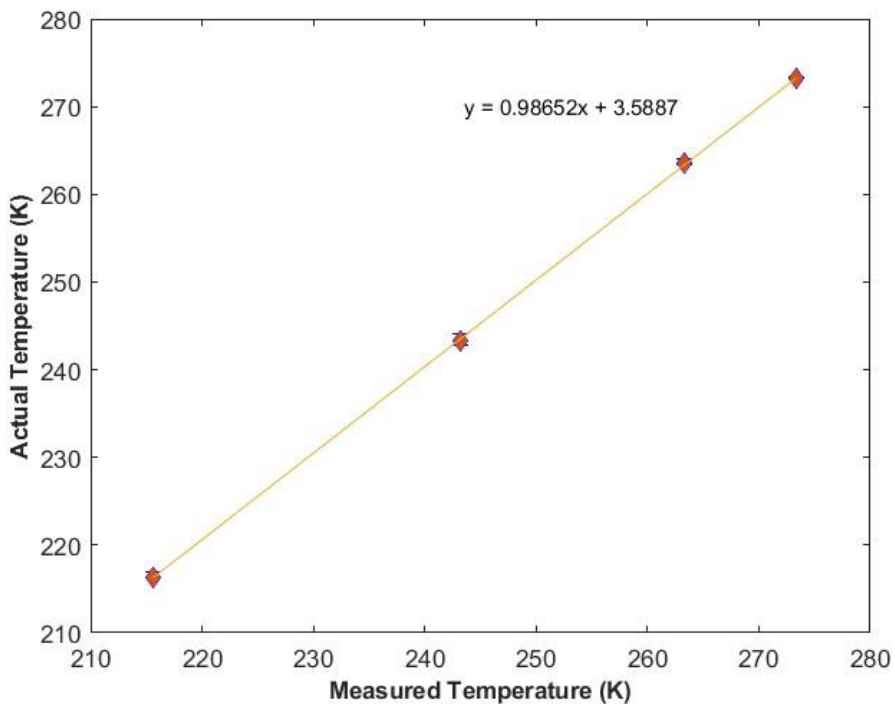


Fig 26. This is the calibration curve that is modeled after the Knopf et al. (2011)³³ study with an $R^2 > 0.9$.

Table 3. Calibration Temperatures of Immersion Freezing Apparatus

Sample	Average T_m (K)	Literature T_m (K)
Water	273.30	273.15
Decane	243.15	243.3 ± 0.6
Dodecane	263.3	263.5 ± 0.3
Octane	215.6	216.3 ± 0.3

Peptide Synthesis

Programs

Ice Recrystallization Inhibition MATLAB Program Script

(Add description here→ make a flow chart?)

References

1. Naing, A. H.; Kim, C. K., A brief review of applications of antifreeze proteins in cryopreservation and metabolic genetic engineering. *3 Biotech* 2019, 9 (9), 329.
2. Surís-Valls, R.; Voets, I. K., Peptidic Antifreeze Materials: Prospects and Challenges. *International Journal of Molecular Sciences* 2019, 20 (20), 5149.
3. Eskandari, A.; Leow, T. C.; Rahman, M. B. A.; Oslan, S. N., Antifreeze Proteins and Their Practical Utilization in Industry, Medicine, and Agriculture. *Biomolecules* 2020, 10 (12).
4. Koshio, K.; Arai, K.; Waku, T.; Wilson, P. W.; Hagiwara, Y., Suppression of droplets freezing on glass surfaces on which antifreeze polypeptides are adhered by a silane coupling agent. *Plos One* 2018, 13 (10).
5. Zhang, Y. F.; Liu, K.; Li, K. Y.; Gutowski, V.; Yin, Y.; Wang, J. J., Fabrication of Anti-Icing Surfaces by Short alpha-Helical Peptides. *ACS Appl. Mater. Interfaces* 2018, 10 (2), 1957-1962.
6. Budke, C.; Koop, T., Ice Recrystallization Inhibition and Molecular Recognition of Ice Faces by Polyvinyl Alcohol. *Chemphyschem : a European journal of chemical physics and physical chemistry* 2006, 7, 2601-6.
7. Zhang, Z.; Liu, X.-Y., Control of ice nucleation: freezing and antifreeze strategies. *Chemical Society Reviews* 2018, 47 (18), 7116-7139.

8. Davies Peter L., Baardsnes Jason, Kuiper Michael J. and Walker Virginia K. Structure and function of antifreeze proteins. *Phil. Trans. R. Soc. Lond.* 2002 B357927–935.
9. Ramløv, H.; Friis, D. S., *Antifreeze Proteins Volume 1*. Springer Nature Switzerland AG: Cham, Switzerland, 2020; Vol. 1.
10. Ramløv, H.; Friis, D. S., *Antifreeze Proteins Volume 1*. Springer Nature Switzerland AG: Cham, Switzerland, 2020; Vol. 2.
11. Davies Peter L., Baardsnes Jason, Kuiper Michael J. and Walker Virginia K. Structure and function of antifreeze proteins *Phil. Trans. R. Soc. Lond.* 2002 B357927–935.
12. Kun, H.; Mastai, Y., Activity of short segments of Type I antifreeze protein. *Biopolymers* 2007, 88 (6), 807-14.
13. Mochizuki, K.; Molinero, V., Antifreeze Glycoproteins Bind Reversibly to Ice via Hydrophobic Groups. *Journal of the American Chemical Society* 2018, 140 (14), 4803-4811.
14. Graether, S. P.; Kuiper, M. J.; Gagné, S. M.; Walker, V. K.; Jia, Z.; Sykes, B. D.; Davies, P. L., β -Helix structure and ice-binding properties of a hyperactive antifreeze protein from an insect. *Nature* 2000, 406 (6793), 325-328.
15. Liou, Y.-C.; Tocilj, A.; Davies, P. L.; Jia, Z., Mimicry of ice structure by surface hydroxyls and water of a β -helix antifreeze protein. *Nature* 2000, 406 (6793), 322-324.
16. Hudait, A.; Odendahl, N.; Qiu, Y.; Paesani, F.; Molinero, V., Ice-Nucleating and Antifreeze Proteins Recognize Ice through a Diversity of Anchored Clathrate and Ice-like Motifs. *Journal of the American Chemical Society* 2018, 140 (14), 4905-4912.
17. Chakraborty, S.; Jana, B., Ordered hydration layer mediated ice adsorption of a globular antifreeze protein: mechanistic insight. *Physical Chemistry Chemical Physics* 2019, 21 (35), 19298-19310.
18. Hudait, A.; Qiu, Y.; Odendahl, N.; Molinero, V., Hydrogen-Bonding and Hydrophobic Groups Contribute Equally to the Binding of Hyperactive Antifreeze and Ice-Nucleating Proteins to Ice. *Journal of the American Chemical Society* 2019, 141 (19), 7887-7898.
19. Hudait, A.; Moberg, D. R.; Qiu, Y.; Odendahl, N.; Paesani, F.; Molinero, V., Preordering of water is not needed for ice recognition by hyperactive antifreeze proteins. *Proc Natl Acad Sci U S A* 2018, 115 (33), 8266-8271.
20. Urbańczyk, M.; Góra, J.; Latajka, R.; Sewald, N., Antifreeze glycopeptides: from

structure and activity studies to current approaches in chemical synthesis. *Amino Acids* 2017, **49** (2), 209-222.

21. Budke, C.; Heggemann, C.; Koch, M.; Sewald, N.; Koop, T., Ice Recrystallization Kinetics in the Presence of Synthetic Antifreeze Glycoprotein Analogues Using the Framework of LSW Theory. *The Journal of Physical Chemistry B* 2009, **113** (9), 2865-2873.
22. Budke, C.; Koop, T., Ice Recrystallization Inhibition and Molecular Recognition of Ice Faces by Polyvinyl Alcohol. *Chemphyschem : a European journal of chemical physics and physical chemistry* 2006, **7**, 2601-6.
23. Knight, C. A.; Wen, D.; Laursen, R. A. Nonequilibrium Antifreeze Peptides and the Recrystallization of Ice. *Cryobiology* 1995, **32**, 23–34.
24. Naullage, P. M.; Molinero, V., Slow Propagation of Ice Binding Limits the Ice-Re-crystallization Inhibition Efficiency of PVA and Other Flexible Polymers. *Journal of the American Chemical Society* 2020, **142** (9), 4356-4366.
25. Congdon, T.; Notman, R.; Gibson, M. I. Antifreeze (Glyco)protein Mimetic Behavior of Poly(vinyl alcohol): Detailed Structure Ice Recrystallization Inhibition Activity Study. *Biomacromolecules* 2013, **14**, 1578–1586.
26. Naullage, P. M.; Lupi, L.; Molinero, V., Molecular Recognition of Ice by Fully Flexible Molecules. *The Journal of Physical Chemistry C* 2017, **121** (48), 26949-26957.
27. Bachtiger, F.; Congdon, T. R.; Stubbs, C.; Gibson, M. I.; Sosso, G. C., The atomistic details of the ice recrystallisation inhibition activity of PVA. *Nature Communications* 2021, **12** (1), 1323.
28. Stubbs, C.; Wilkins, L. E.; Fayter, A. E. R.; Walker, M.; Gibson, M. I., Multivalent Presentation of Ice Recrystallization Inhibiting Polymers on Nanoparticles Retains Activity. *Langmuir* 2019, **35** (23), 7347-7353.
29. Zhang, M.; Qiu, Z.; Yang, K.; Zhou, W.; Liu, W.; Lu, J.; Guo, L., Design, synthesis and antifreeze properties of biomimetic peptoid oligomers. *Chemical Communications* 2023, **59** (46), 7028-7031.
30. Delesky, E. A.; Garcia, L. F.; Lobo, A. J.; Mikofsky, R. A.; Dowdy, N. D.; Wallat, J. D.; Miyake, G. M.; Srubar III, W. V., Bioinspired Threonine-Based Polymers with Potent Ice Recrystallization Inhibition Activity. *ACS Applied Polymer Materials* 2022, **4** (10),

7934-7942.

31. Damalanka, V. C.; Voss, J. J. L. P.; Mahoney, M. W.; Primeau, T.; Li, S.; Klampfer, L.; Janetka, J. W., Macrocyclic Inhibitors of HGF-Activating Serine Proteases Overcome Resistance to Receptor Tyrosine Kinase Inhibitors and Block Lung Cancer Progression. *Journal of Medicinal Chemistry* 2021, 64 (24), 18158-18174.
32. Burkey, A. A.; Riley, C. L.; Wang, L. K.; Hatridge, T. A.; Lynd, N. A., Understanding Poly(vinyl alcohol)-Mediated Ice Recrystallization Inhibition through Ice Adsorption Measurement and pH Effects. *Biomacromolecules* 2018, 19 (1), 248-255.
33. Knopf, D. A.; Forrester, S. M. Freezing of Water and Aqueous NaCl Droplets Coated by Organic Monolayers as a Function of Surfactant Properties and Water Activity. *The Journal of Physical Chemistry A* 2011, 115, 5579-5591.